Sains Malaysiana 41(7)(2012): 879–884

Effects of Inter-electrode Gap and Discharge Voltage on EUV Emission from Stainless Steel Vacuum Spark Plasma

(Kesan Ruangan Antara-Elektrod Dan Voltan Nyahcas Terhadap Pancaran EUV daripada Plasma Percikan Vakum Keluli Tahan Karat)

S. SABOOHI, S.L. YAP, L.S. CHAN & C.S. WONG*

ABSTRACT

The emission of Extreme Ultra Violet (EUV) from plasma produced by vacuum spark discharge using stainless steel as anode material was investigated. The operating pressure for all the experiments carried out was maintained at below 10^{-4} mbar. The discharge voltage tested was from 8 kV to 20 kV. The inter-electrode distance suitable for high intensity and reproducible EUV emissions was found to be in the range of 2.6 mm to 4.6 mm. The output EUV energy scaled as ~ V_0^2, where V_0 is the discharge voltage.

Keywords: Extreme Ultra Violet (EUV); vacuum spark

ABSTRAK

Pancaran Ultra Violet lampau (EUV) yang dihasilkan oleh plasma daripada percikan pelepasan vakum yang menggunakan anod yang diperbuat daripada keluli tahan karat telah dikaji. Tekanan operasi untuk kesemua eksperimen dikekalkan di bawah 10^{-4} mbar. Voltan nyahcas diubah daripada 8 kV hingga 20kV. Jarak elektrod yang sesuai untuk pancaran EUV yang tinggi lalah antara 2.6 mm dan 4.6 mm . Tenaga EUV yang dihasilkan ditunjukkan dalam skala ~ V_0^2 dengan V_0 ialah voltan nyahcas.

Kata kunci: Ultraviolet lampau; vakum percikan

INTRODUCTION

The vacuum spark is known to be an excellent pulsed X-ray source covering spectral range that is typical of highly ionized metallic plasmas (Lie et al. 1971; Morita & Fujita 1983; Negus & Peacock 1979; Wong & Lee 1984; Wong et al. 1995). The pulsed plasma is formed between two properly shaped electrodes by the discharge of electrical energy initially stored in a capacitor. The electron temperature of the plasma produced had been reported (Negus et al. 1979) to be in the range of 4 keV to 7 keV, while the electron density is in the range of 10^{21} cm^{-3} to 10^{22} cm^{-3}, which is near to the condition at the core of the Sun. Highly ionized metallic species such as Fe XXVI and Ni XXVII (Fraenkel & Schwan 1972) can be produced by the vacuum spark discharge. For this reason, the vacuum spark had been utilized as a spectroscopic source for laboratory studies of the solar flare phenomena (Lie et al. 1971). In view of the high temperature that can be achieved, there had also been one attempt to operate the vacuum spark with lithium deuterated anode tip as a fusion generating device (Lee & Elton 1976). Recently, this device is being considered as one of the possible EUV sources for Next Generation Lithography (NGL) (Guo et al. 2001; Koshelev et al. 2007; Wyndham et al. 2005).

Ideally, the EUV source required for lithography is expected to be a point source of less than 1 mm^2 in dimension; with in-band radiation output power of about 50 W and can be operated continuously for long duration. The plasma required is believed to have electron temperature below 100 eV so that the emission spectrum is concentrated in the EUV region. As a rule of thumb, the peak of the continuum of the emission spectrum of plasma (Bremsstrahlung and recombination) with electron temperature of 46 eV is expected to be at around 13.5 nm, the in-band wavelength required by the industry. In order to enhance the intensity of EUV emission, it may be more effective to heat the plasma to slightly higher temperature so that a broader temporal width of the EUV emission pulse can be obtained. Since recombination emission is expected to be the dominant continuum emission mechanism at relatively low temperature, and the free-bound emission intensity is proportional to the forth power of the charge number of the ionic species in the plasma, it is an obvious advantage to employ a high Z plasma for this purpose. For line radiation at and near the in-band emission, it is dependent on the ionic species. This can also be one of the important considerations in the effort to enhance in-band EUV emission from plasma.

As a first step towards the development of the vacuum spark device as a EUV source for nanolithography, it is important to determine the suitable experimental parameters for consistent operation of the device. In the work reported here, the effects of various experimental parameters of the vacuum spark discharge on its EUV emission have been investigated. In particular, the discharge voltage and inter-electrode separation was found to be the most important parameters in determining the performance of the vacuum spark as a EUV source.

EXPERIMENTAL SETUP

The vacuum spark system used in this work is similar to that described in earlier publication (Chew & Wong 2006). It is powered by a single 1.85 μF Maxwell energy storage capacitor, which can be charged up to a maximum voltage of 60 kV and having an internal inductance of 15 nH. The vacuum spark discharge system consists of a stainless steel hollow cathode and a replaceable anode that is also made of stainless steel. The discharge chamber is evacuated to a pressure of lower than 10^{-4} mbar by using a diffusion pump backed by a rotary pump. The gap between the electrodes can be varied by adjusting the position of the anode. Upon triggering, electrons from the spark formed between the triggering pin and the cathode plate are accelerated towards the anode under the effect of the high electric field across the inter-electrode vacuum gap prior to electrical breakdown. The bombardment of electrons at the anode will vaporize it and subsequently will be heated by the discharge to form hot dense metallic plasma that is capable of emitting in the UV, EUV, soft X-ray and hard X-ray regions depending on the condition of the plasma (Wong et al. 1995).

The vacuum spark system is shown schematically in Figure 1. A magnetic probe is employed to monitor the time variation of the discharge current. To monitor the time evolution of the EUV emission, a silicon photodiode with integrated multilayer filter of silicon and zirconium to give a pass band of 11 nm to 18 nm (IRD Inc. SXUV-5A Si/Zr 100/200 nm) is employed. The sensitivity of this detector is 95 mA W^{-1} at wavelength around 13 nm (peak). The X-ray emission is measured by a PIN diode covered with a 24 μm thick aluminized Mylar film. This detector is sensitive to wavelength in the range of 3 to 30 Å. The response curves (amperes per watt of radiation detected against wavelength) for the two detectors are shown together in Figure 2.

The plasma produced by the stainless steel vacuum spark discharge emits both continuum and characteristic line radiations that cover a wide range of wavelengths extending from the visible, UV, EUV, soft X-ray and to hard X-ray region. Experiments have been carried out with discharge voltages in the range of 8 kV to 20 kV, corresponding to electrical input energies of 59.5 J to 370 J, respectively. The operating pressure for all the experiments is maintained at less than 10^{-4} mbar. The inter-electrode gap distance d is varied from 1.6 mm to 6.7 mm. It is found that beyond this range of d, the EUV emission output becomes insignificantly low.

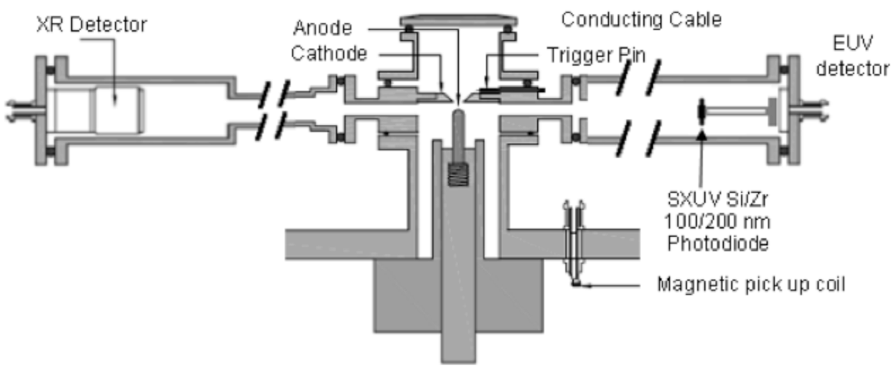

FIGURE 1. Schematic diagram of the vacuum spark system

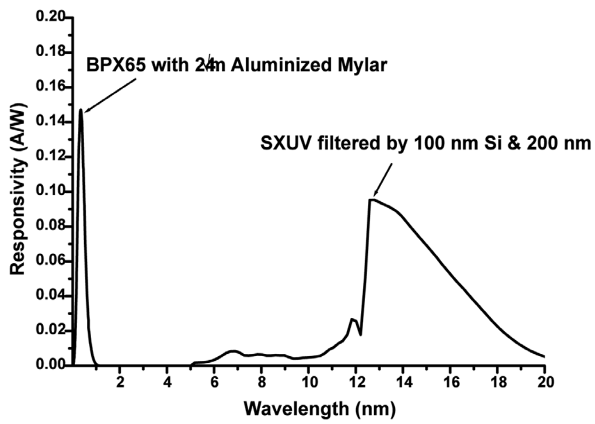

FIGURE 2. Responsivity curves of BPX65 PIN diode (with 24 μm aluminized Mylar) plotted together with that of SXUV p-n junction diode with 100 nm Si and 200 nm Zr

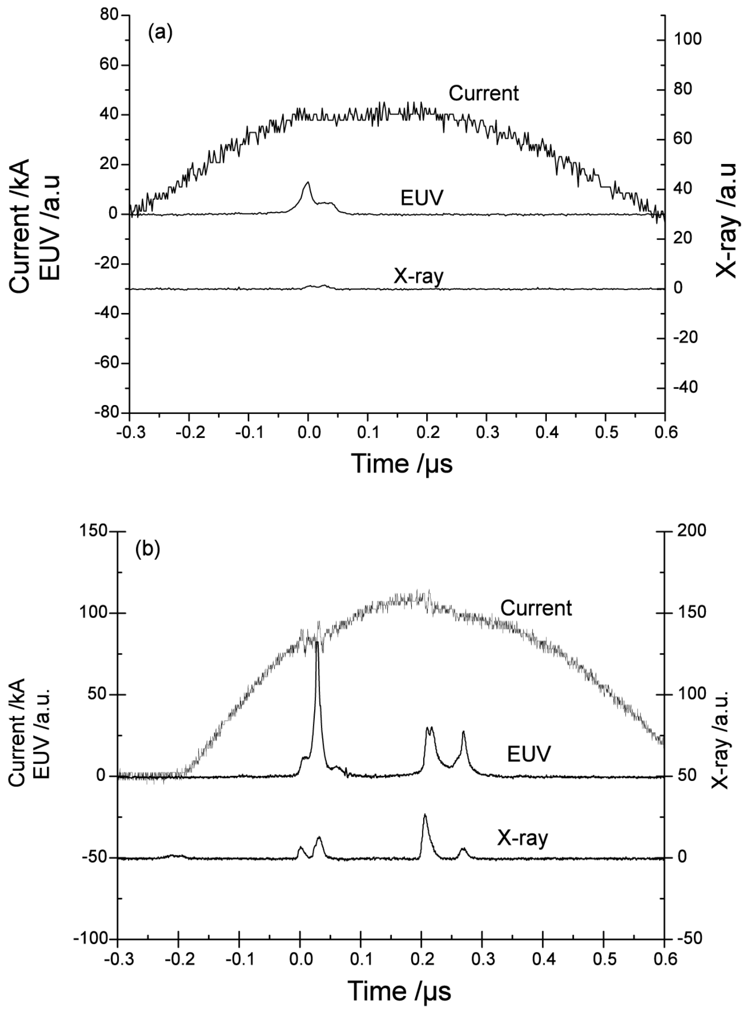

FIGURE 3. Typical vacuum spark discharges with inter-electrode separation of 2.6 mm and discharge voltage of (a) $V_0 = 8$ kV; and (b) $V_0 = 20$ kV

RESULTS AND DISCUSSION

Figure 3 shows the time evolution of the discharge currents, the x ray and EUV emissions of typical discharges at discharge voltages of $V_0 = 8$ kV and 20 kV for inter-electrode separation of $d = 2.6$ mm.

The discharge current waveform for both cases shows a current dip indicating the occurrence of pinch phenomenon. The EUV emission is observed to be well aligned with the current dip. In the case of 8 kV discharge, the current dip is observed at around 450 ns after the start of the discharge while for 20 kV discharge, it occurs at around 200 ns after the start of the discharge. A much stronger pinch is expected for the case of 20 kV discharge as indicated by the more severe dip in the current. The pinch is seen to occur at discharge current of about 100 kA as compared to the case of 8 kV discharge, which is only about 50 kA. The corresponding amplitudes of EUV emissions are also consistent with this observation, with 80 (arbitrary unit) in the case of 20 kV discharge as compared to 15 in the case of 8 kV discharge. For discharges at 20 kV, X-ray signal is also registered by the PIN diode simultaneously with the EUV signal. Moreover, the time of occurrence of the pinch is also observed to be shorter for higher discharge voltage. This is consistent with the fact that with higher discharge current, the pinching will be faster and stronger thus leading to the formation of a hotter plasma and subsequently rapid development of instability. With slower and weaker pinching as in the case of lower discharge voltage, the final pinch column is formed after the peak of the discharge current, with no evidence of instability. It is possible that the column will just expand after it reaches a minimum radius since the current is then decreasing.

The strong dependence of the EUV intensity on the capacitor discharge voltage is obvious in the comparison of Figure 3(a) and 3(b). For discharges below 8 kV, the EUV emission is found to be negligibly low.

In order to determine the optimum inter-electrode distance for consistent and high intensity EUV output, a series of experiments have been carried out to measure the EUV emission intensity for various combinations of V_0 and d in the ranges of $V_0 = 8$ to 20 kV and $d = 1.6$ to 6.7

mm. The relative EUV energy emitted from the discharges performed were estimated from the areas under the EUV pulses detected. The comparison of relative EUV energy emitted from the above series of discharges is shown in Table 1 and plotted as shown in Figure 4. From these data, it is clear that for the present vacuum spark system, the range of inter-electrode distance for best performance is between 2.6 mm and 4.6 mm. For the particular inter-electrode distance of 2.6 mm, a logarithmic plot of output EUV energy against the discharge voltage as shown in Figure 5 gives a straight line with gradient of 1.968, which reveals that the output EUV energy scales as V_0^2, or directly proportional to the electrical input energy. This implies that the output EUV energy of the device can be increased by increasing the electrical input energy.

Figure 6 illustrates the shot-to-shot variation of the EUV emission over 55 discharges of the vacuum spark with V_0 = 20 kV and d = 2.6 mm. The relative EUV emission output energy is observed to fluctuate about an average (arb. unit) of 0.8 with a mean deviation of ± 0.2, which can be considered to be reasonably reproducible.

CONCLUSION

The inter-electrode separation was shown to play an important role in the vacuum spark discharge that affect the condition of the plasma and consequently on the EUV emission output. The inter-electrode separation for high intensity and consistent EUV emission was found to be in the range of 2.6 mm to 4.6 mm. For the present system, the highest EUV output is obtained at an inter-electrode separation of 2.6 mm and discharge voltage of 20 kV. The EUV output is shown to scale with discharge voltage as ~V_0^2, or directly proportional to the electrical input energy.

TABLE 1. Average output EUV energy (arb unit) of vacuum spark discharges at various discharge voltages and inter-electrode separations

	8 kV	10 kV	12 kV	15 kV	20 kV
d = 6.7 mm	-	8.61E-03	2.46E-03	3.22E-03	-
d = 6.2 mm	2.96E-03	1.01E-02	1.07E-02	4.01E-03	-
d = 5.7 mm	3.87E-03	4.19E-03	9.20E-03	7.83E-03	-
d = 4.6 mm	1.63E-01	2.74E-01	3.69E-01	6.32E-01	6.96E-01
d = 3.6 mm	1.78E-01	2.21E-01	4.13E-01	6.48E-01	8.05E-01
d = 2.6 mm	1.93E-01	3.16E-01	4.28E-01	6.54E-01	8.77E-01
d = 2.1 mm	1.70E-01	2.30E-01	2.59E-01	3.80E-01	4.14E-01
d = 1.6 mm	9.13E-02	9.83E-02	7.18E-02	1.56E-01	3.62E-01

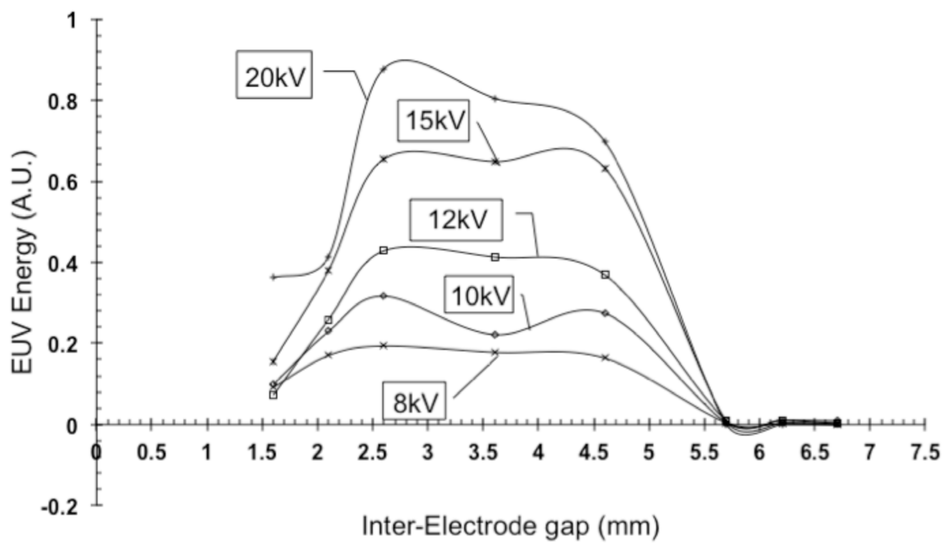

FIGURE 4. Average output EUV energy for different discharge voltages (from 8 kV to 20 kV) and inter-electrode separations (from 1.6 mm to 6.7 mm)

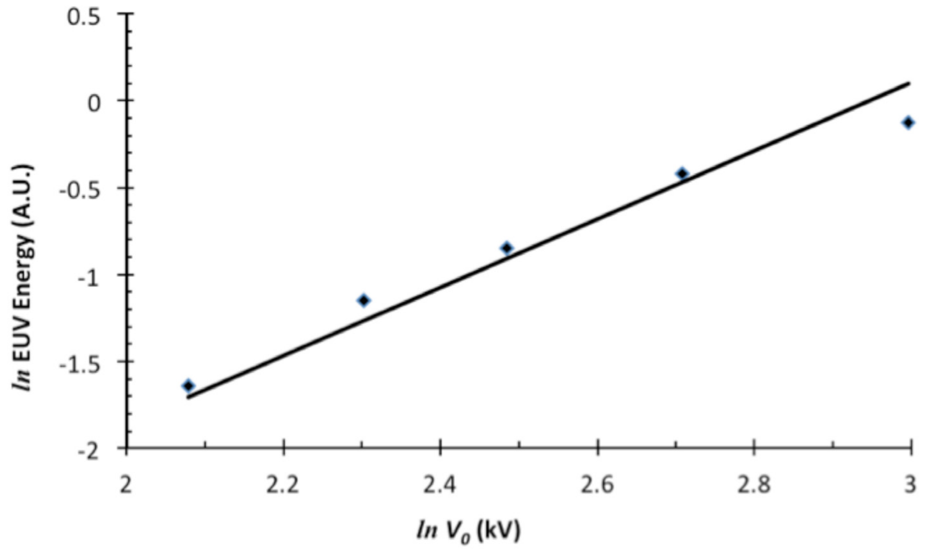

FIGURE 5. Logarithmic plot of output EUV energy against discharge voltage for inter-electrode distance of 2.6 mm

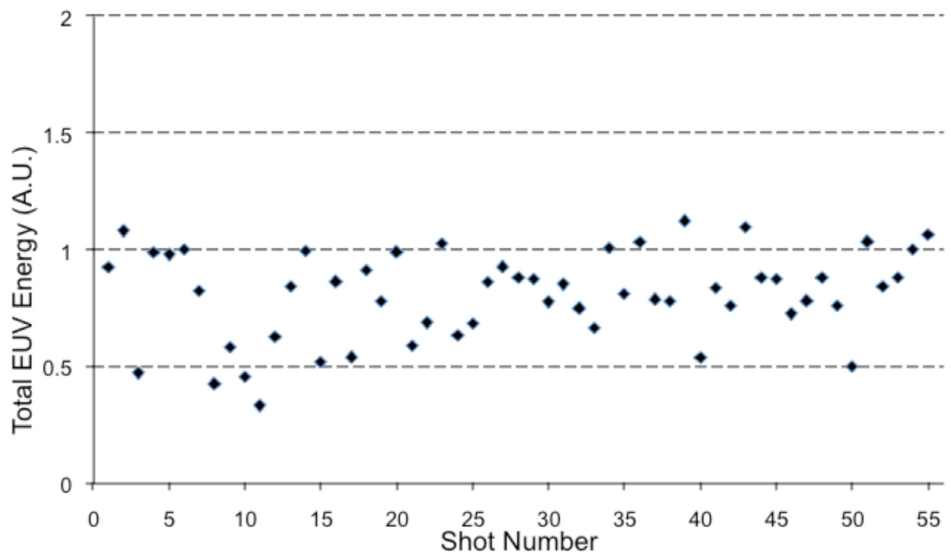

FIGURE 6. Shot-to-shot variation of EUV emission over 55 discharges with $V_0 = 20$ kV and $d = 2.6$ mm

ACKNOWLEDGEMENT

This project was partially supported by the Toray Research Grant awarded to the University of Malaya (MTSF1045-2009A), and University of Malaya research grants (RG084-09AFR, PS219-2009A and PS330-2010A). The authors are grateful to Mr. Jasbir Singh for technical support.

REFERENCES

Chew, S.H. & Wong, C.S. 2006. X-Ray and EUV emission characteristics of a vacuum spark. *Journal of Science and Technology in the Tropics* 2: 125-129.

Fraenkel, B.S. & Schwob, J.L. 1972. X-ray spectra of highly ionised iron and nickel atoms. *Physics Letters A* 40: 83-85.

Guo, Xiaoming, Xu, Meisheng, Ye, Rubin, Huang, Chaofeng, Wirpszo, K.W. & Panarella, Emilio. 2001. A Vacuum Spark Point Source for X-ray/EUV lithography. *Proceedings of SPIE* 4343: 491-496.

Koshelev, K.N., Banine, V.E. & Salashchenko, N.N. 2007. Research and development in short-wave radiation sources for new-generation lithography. *Physics-Uspekhi* 50: 741-744.

Lee, S. & Conrads, H. 1976. Measurement of neutrons and X-rays from a vacuum spark, *Physics Letters A* 57: 233-236.

Lie, T.N. & Elton, R.C. 1971. X Radiation from Optical and inner-shell transitions in a highly ionized dense plasma. *Physical Review A* 3: 865-871.

Morita, S. & Fujita, J. 1983. Spatially resolved $K\alpha$ spectra of two-structure plasmas in a vacuum spark. *Applied Physics Letter* 43: 443-445.

Negus, C.R. & Peacock, N.J. 1979. Local regions of high-pressure plasma in a vacuum spark. *Journal of Physics D: Applied Physics* 12 : 91-111

Wong, C.S. and Lee, S. 1984. Vacuum spark as a reproducible x ray source. *Review of Scientific Instruments* 55: 1125-1128.

Wong, C.S., Ong, C.X., Moo, S.P. & Choi, P. 1995. Characteristics of a Vacuum Spark Triggered by the Transient Hollow Cathode Discharge Electron Beam. *IEEE Transactions on Plasma Science* 23: 265-269.

Wyndham, E.S., Favre, M., Chuaqui, H., Choi, P., Leñero, A.M. & Díaz, J.S. 2005. Reproducibility of a titanium plasma vacuum spark discharge. *IEEE Transactions on Plasma Science* 33:1662-1667.

Plasma Technology Research Centre
Department of Physics
Faculty of Science
University of Malaya
50603 Kuala Lumpur
Malaysia

*Corresponding author; email: cswong@um.edu.my

Received: 21 October 2011
Accepted: 3 February 2012